Supporting Information

A novel heat storage ionomer binder for thermal management of Li-ion batteries

Danni Shen[a], Tingting Han[e], Jie Liu[b, *], Junwu Yang[e], Jinqiu Zhou[b], Yufei Li[d], Xi Zhou[b, f], Zhenkang Wang[a], Tao Qian[b], Chenglin Yan[a, c, f, *]

[a] College of Energy, Soochow University, Suzhou 215006, China

[b] College of Chemistry and Chemical Engineering, Nantong University, Seyuan 9, Nantong 226019, China

[c] School of Petrochemical Engineering, Changzhou University, Changzhou 213164, China

[d] Pinghu Institute of Advanced Materials, Zhejiang University of Technology, Pinghu 314200, China

[e] State Key Laboratory of Space Power-sources Technology, Shanghai Institute of Space Power-Sources, 2965 Dongchuan Road, Shanghai 200245, China

[f] Key Laboratory of Core Technology of High Specific Energy Battery and Key Materials for Petroleum and Chemical Industry, Soochow University, Suzhou, 215123, China

* Corresponding authors

E-mail addresses: jliu93@ntu.edu.cn (J. Liu); c.yan@suda.edu.cn (C. Yan)

Experimental Section

Materials

Polyethylene glycol (PEG, M_w = 10000, Richjoint), Tannic acid (TA, Macklin), anhydrous ferric chloride ($FeCl_3$, Sinopharm) and N-methyl pyrrolidone (NMP, Sinopharm) were used as received without further purification. The commercial carbonate-based liquid electrolyte composed of 1 M $LiPF_6$ in ethylene carbonate (EC)/diethyl carbonate (DEC) (EC/DEC = 1:1, by volume) was purchased from DoDoChem..

Fabrication of HSIB

HSIB was simply fabricated by mixing PEG, TA and $FeCl_3$ aqueous solution. First, PEG and TA were blended under stirring and 80 °C oil bath, with moderate deionized water and ethanol as solvent. After uniformly mixed, $FeCl_3$ which had been dissolved in deionized water was added into the mixture subsequently. Keep stirring and heating for 24 h to remove the solvent. After being cooled to room temperature (T_{room}), HSIB was got. Besides, the mixture of PEG and TA fabricated by the above-mentioned method is denoted as Intermediate, which is not containing any Fe^{3+}. In this work, the mass ratio of PEG and TA is 5:1, and the mole ratio of TA and Fe^{3+} is 3:5.

Fabricate of the LFP cathode

To greatly compare the thermal property and electrochemical property between the HSIB, polyvinylidene fluoride (PVDF) and pure PEG, we fabricated the cathode with $LiFePO_4$ (LFP) as cathode active material, conductive acetylene black (AB) as conductive agent, and HSIB, PVDF or PEG as binder, NMP as solvent. The slurry of LFP, binder and AB was casted onto aluminum foil and dried in a vacuum oven under 80 °C for 12 h.

Characterizations

The formation of HSIB

Fourier transform infrared spectrometry (FTIR, Tensor 27, Bruker) and Resonance Raman spectra (HR Evolution, Horiba Jobin Yvon) measurements were used to analysis the chemical structure of HSIB. The FTIR spectra of HSIB was obtained with attenuated total refraction (ATR) instrument and the others were tested as KBr disks. Raman spectra was obtained with 633 nm excitation. Ex-situ X-ray diffraction (XRD, D8 Advance, Bruker) were measured to characterize the

crystal structure change of the fabrication processes of the ionomer, while in-situ X-ray diffraction was used to verify the crystal structure and crystallinity change by temperature.

The thermal property

Differential scanning calorimetry (DSC, METTLER TOLEDO, Switzerland) was used to characterize the thermal property of binders and the resulted cathode materials. Thermal imager (FLIR E4 WiFi, FLIR Systems OÜ, Estonia) was employed to visualize the temperature variation of the heated cathodes or pouch cells.

Nail test

To simulate the practical effect of HSIB on controlling the temperature rise of batteries when violent internal short circuit occurs, we performed the nail test. To reduce the errors induced by battery performance differences and the packaging process, the resulted pouch cells undergone 2 cycles of discharging to 2.5 V and charging for 30 minutes, with a 400 mA h current density. After that, the temperature of the cells could easily exceed the phase transition temperature of HSIB after being pierced but won't cause serious fire or explosion. For all the used pouch cell in this work, the time that the second discharge process cost is 30 ± 0.5 min, and the charge/discharge curve is smooth.

Thermal model

Thermal simulation was employed to confirm practical effect of HSIB under cycles. The structure of cell was simplified with a lumped parameter model, and the thermal effect of cell was deducted by finite element simulation using Comsol Multiphysics. The special heat capacity data derives from the DSC data of cathode materials in Fig. 2(d).

The electrochemical property

The long-cycle and rate performance were tested in a voltage range of 2.5–4.0 V (vs. Li^+/Li) using a LAND system (CT 2001A, Wuhan, China). Cyclic voltammetry (CV) and electrochemical impedance spectrum (EIS) measurements were conducted on an electrochemical workstation (CHI660E, Wuhan, China), in which CV was tested in a potential window of 2.5–4.0 V (vs. Li^+/Li) at 0.5 mV s^{-1} and EIS was measured in a frequency range of 0.01 Hz–1 MHz.

All the coin cell in this work were 2025 type and assembled in an Ar-filled glove box with both O_2 and H_2O are less than 0.1 ppm. The separator adopted in SS||SS coin cell is cellulose, and the others are PP.

The temperature alternation test

To explore the effects of temperature changes on the cell performance of HSIB and PVDF, we designed the temperature variation test. At the first, two kinds of LFP half-cells are operated for 10 cycles in 1 C and T_{room} to select the cells with similar capacity and stability. Then, the cells were placed in an oven for the single cycle temperature alternating. To ensure the cells could be completely heated or cooled, the interval of 20 min of each alternating was selected. And a current density of 40 mA h g^{-1} was chosen at aim of undergoing at least 10 times of temperature alternating. After that, the cells were cycled in 170 mA h g^{-1} under shifted temperature for cycles to explore the performance in different temperature. Finally, the cells were kept in T_{room} for cycles.
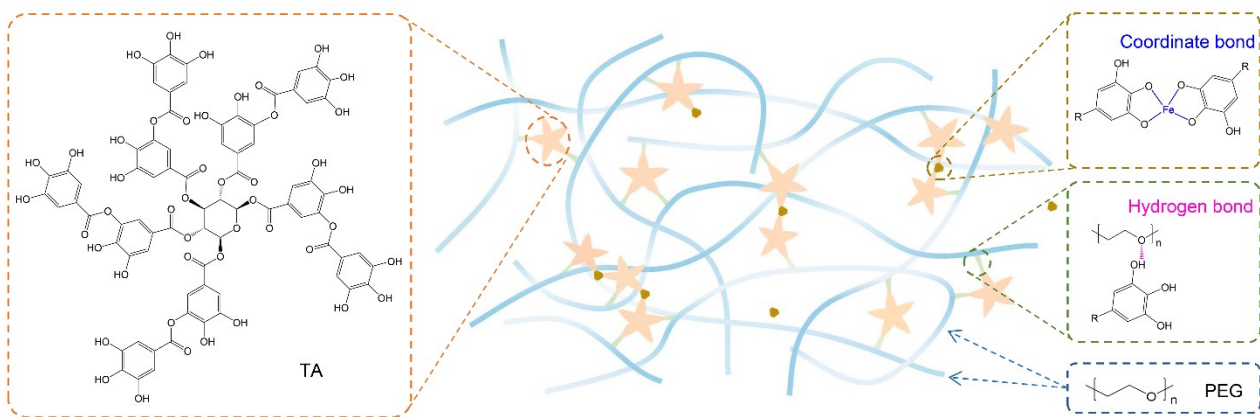
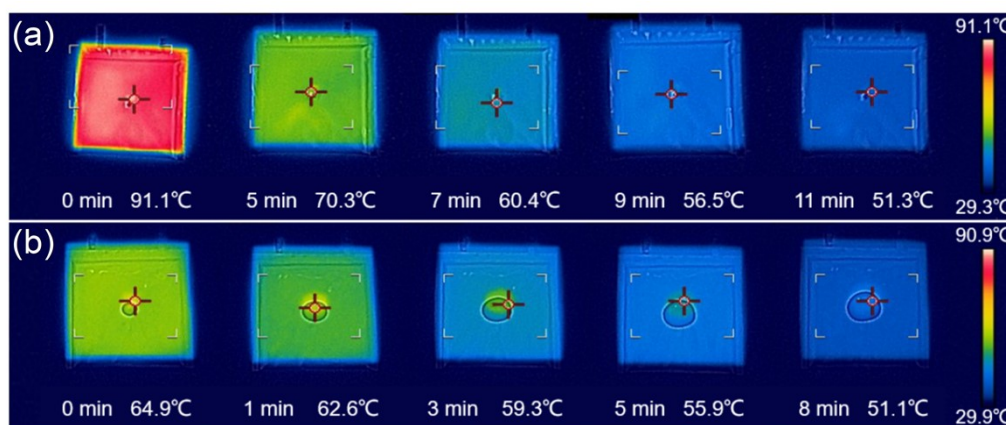**Fig. S1** Schematic illustration of the interaction of PEG, TA and Fe3+ in HSIB.

Fig. S2 The cooling process of the LFP pouch cell with (a) PVDF and (b) HSIB after nailing.
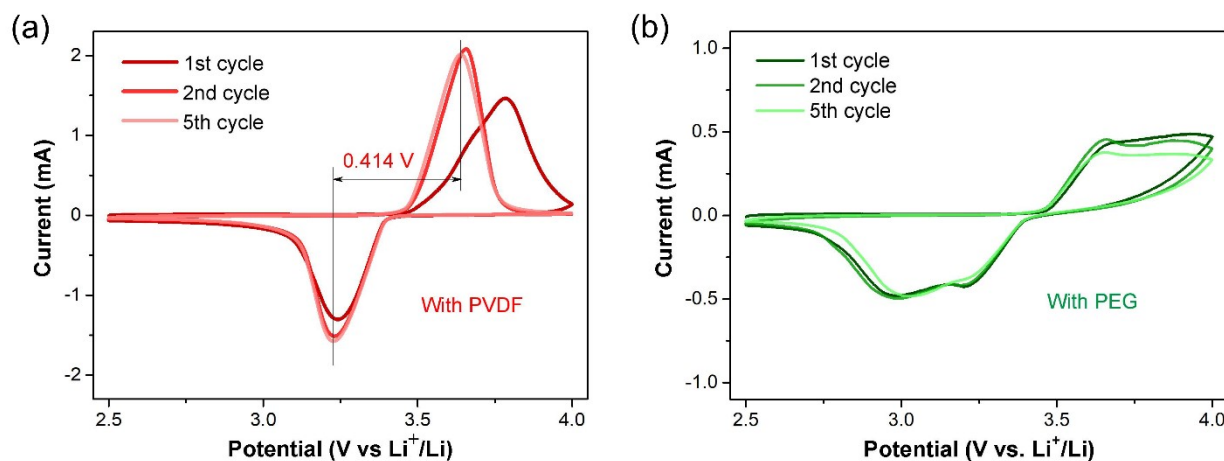

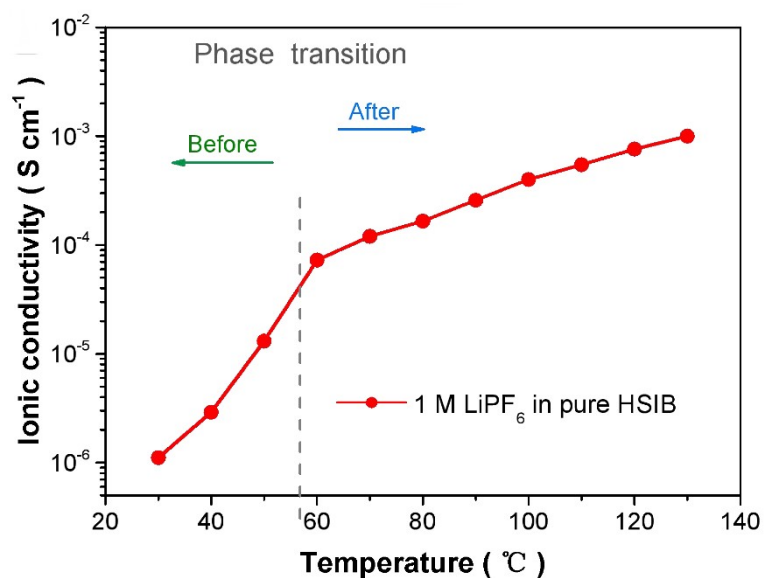**Fig. S3** The CV curves for LFP||Li half cells with (a) PVDF and (b) PEG cathodes, the sweep rate is 0.5 mV s^{-1}.
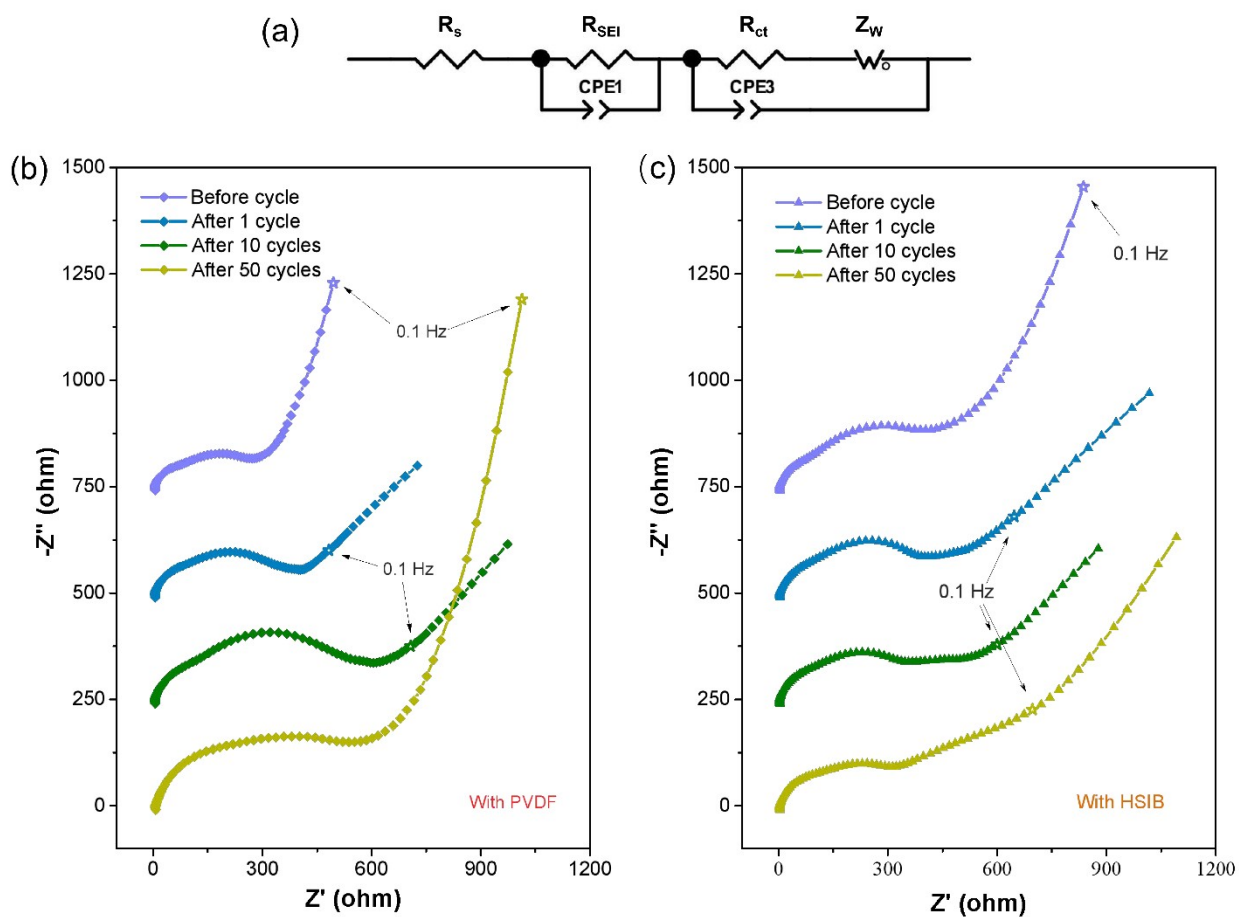
Fig. S4. Ionic conductivity of HSIB.

Fig. S5 (a) The equivalent circuit diagram of the assembled half cells with PVDF and HSIB cathodes. EIS measurements for the LFP‖Li half cells with (b) PVDF and (c) HSIB cathodes before and after cycles.
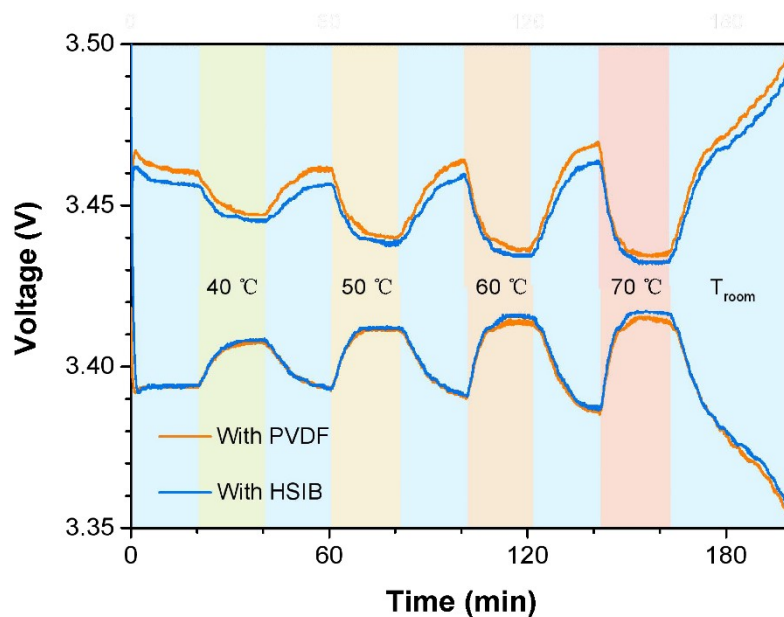
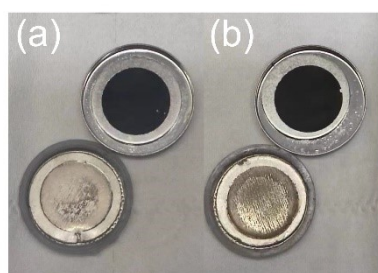**Fig. S6** The median voltage of the PVDF and HSIB half-cells in single cycle temperature alternation.

Fig. S7 Photograph of electrodes with (a) HSIB and (b) PVDF after temperature alternation test.

Table S1 Physical parameters of the 3D model for thermal simulation.[1]

Parameter	Al	Cathode	Cu	Anode	Separator	Electrolyte
L (μm)	10	50	10	30	25	-
ρ (kg m^{-3})	2700	1500	8960	2660	492	1210
λ (W m^{-1} K^{-1})	238	1.48	400	1.04	0.334	0.099
C$_p$ (J kg^{-1} K^{-1})	900	-	385	1437.4	1978	1518

Table S2 Result of thermal simulation.

Time (min)	$T_{\text{PVDF-Model}}$ (°C)	$T_{\text{HSIB-Model}}$ (°C)	ΔT (°C)	Ratio of temperature decrease
0	30	30	0	0.00%
5	36.917	34.904	2.013	29.10%
10	42.144	38.635	3.509	28.89%
15	48.375	42.964	5.411	29.45%
20	53.072	46.298	6.774	29.36%
25	58.981	50.399	8.582	29.61%
30	63.367	53.495	9.872	29.59%
35	69.056	57.333	11.723	30.02%
40	73.228	60.102	13.126	30.36%
45	78.757	63.437	15.32	31.42%
50	82.77	65.456	17.314	32.81%
55	88.186	67.318	20.868	35.86%
60	92.099	69.554	22.545	36.30%
65	97.433	73.446	23.987	35.57%
70	101.25	76.29	24.96	35.03%

Table S3 The resistance data of equivalent circuit fit of the EIS measurements for the HSIB half-cell.

		R_b	R_{SEI}	R_{ct}
HSIB	Before cycle	2.103	145.1	544.6
	1st cycle	1.238	182.1	446.6
	10th cycle	1.108	178.2	434.8
	50th cycle	2.251	180.9	477.8
PVDF	Before cycle	3.465	133.3	337.3
	1st cycle	3.844	188.8	396.8
	10th cycle	3.849	237.8	548.5
	50th cycle	6.205	374.4	933.2

Reference

1. C. X. He, Q. L. Yue, M. C. Wu, Q. Chen and T. S. Zhao, *Int. J. Heat Mass Transfer*, 2021, **181**, 121855.